ACERP: Vol. 4, No.2, (Spring 2018) 16-26

Advanced Ceramics Progress

Research Article

Journal Homepage: www.acerp.ir

An investigation on injectable composites fabricated by 45S5 bioactive glass and gum tragacanth: Rheological properties and in vitro behavior

Mahtab Rasti, Saeed Hesaraki*, Nader Nezafati

Department of Nanotechnology & Advanced Materials, Materials and Energy Research Center, Karaj, Iran.

PAPER INFO

Paper history:
Received 09 September 2018
Accepted in revised form 20 January 2019

Keywords:
Injectable composite
Tragacanth
45S5 bioactive glass
Rheological properties
Degradability
Swelling

ABSTRACT

The injectable composites were formulated from melt-derived 45S5 bioactive glass powder and gum tragacanth. The effect of the tragacanth (2 and 4 w/v%) and powder to liquid ratio (P/L= 1.5 to 2.5) on rheological properties, injectability, degradation, swelling, and bioactivity the composites were studied. With increasing the P/L ratio and tragacanth concentration, the force required for injection of the composites is increased. However, the formulated composites show maximum injection force of 15 N, which seems to be appropriate for surgical purposes. The formulated composites indicate positive thixotropic behavior, whereas increasing tragacanth from 2% to 4% lead to deteriorating its behavior. Moreover, thecomposites formulated by 2% tragacanth show much more resistance against degradation and swelling. The bioactivity analyze confirms the formation of flake-like apatite nanostructures on the surface of nanocomposites in initial days of immersion into the SBF solution.

1. INTRODUCTION

In recent years, the injectable composite biomaterials have been increasingly popular for tissue engineering, particularly bone repair and regeneration because of their advantages including ease of handling and application without any requirement for open surgery, the ability of filling defects with irregular shapes, and diminished treatment costs and time. The injectable composite biomaterials are composed of organic and inorganic parts [1, 2]. The inorganic components comprise ceramic or glass particles dispersed within the organic matrix. The inorganic particles induce the bioactivity whereas the organic matrix acts as a carrier as well as stimulates the flowability and plasticity of the composite [3].

Bioactive glasses are a category of the biomaterials that can be transplanted into both hard and soft tissues. The main components of the bioactive glasses are as follows: SiO_2, Na_2O, CaO, and P_2O_5. The first bioactive glass compound ($45SiO_2$, $24.5Na_2O$, 24.4CaO, $6P_2O_5$) has been introduced by Hench et al. in 1972, which is commercially available as 45S5 Bioglass® [4]. The common characteristic of the bioactive glasses is time-dependent reactions on their surface that occurs during their implantation into the body. In fact, the bioactivity is an intermediate state between complete dissolution and neutrality by which a nanostructured layer of hydroxyapatite is formed on the surface of the glasses.This layeris biologically active and satisfies the chemical bonding with the tissue [5].

The bioactive glasses have been successfully utilized as a bone filler for orthopedics and dental surgery. Their outstanding properties like desirable bioactivity, osteoconductivity, osteoinductivity, and biodegradability make them as a promising candidate for biomedical engineering [5]. The bioactive glasses release a specified amount of ions such as Ca^{2+},PO_4^{-3}, Na^+ and Si^{4+}, which are essential for bonding and regeneration of the bone. However, the bioactive glasses suffer from low mechanical strength and toughness due to the presence of the amorphous glass network. The tensile and flexural strength of the bioactive glass compounds is in the range of 40 to 60 MPa, resoectively. They are therefore not suitable for load-bearing applications and is just recommended to use them as the bioactive fillers in the composites [6].

There are a number of polymeric materials, which are capable of using as an organic component of the injectable composite materials. It should be mentioned that a natural polymer is a complex mixture of soluble

* *Corresponding Author's Email: s.hesaraki@merc.ac.ir (S. Hesaraki)*

and insoluble polysaccharides in water along with a small amount of protein, starch, and cellulosic material [7]. Excellent chemical and biological properties of the natural polymers have made them as the promising candidates to be practically served in the chemical and environmental engineering, agriculture, food industry, and medicine [8]. Today, using the natural polymers in biomedicine has been considered because of non-toxicity, biodegradability, biocompatibility, affordability, and availability. In this regard, various types of natural polysaccharideslike chitosan, alginate, dextran, starch, gelatin, pectin, guar gum, xanthan, cellulose and carrageenan, are used as the nanostructured systems including nanofilms, nano-fibers and nanoparticles for wound dressings, medical implants, drug delivery systems, vascular connections, and new tissue engineering scaffolds [9, 10].

Gum tragacanth is a natural anionic hydrocolloid composed of two polysaccharides, bassorin, and tragacanthin. Tragacanthin is the major component of the tragacanth, which is highly water soluble and forms a mucilaginous colloid. Bassorin has a low solubility in water but it can swell to createa gel. Consequently, tragacanth can act either as a thickening agent and/or emulsifier, so, it can beknown as a bifunctional emulsifier [11]. The gum has been used in traditional medicine as the burn ointment and ulcer cream, which has several advantages such asincreasingthe wound healing rate,improvingthe formation of granular tissue and restoringmucosa. Furthermore, the gum tragacanth is used as a suspending agent in the pharmaceutical industry to prevent the sedimentation of the insoluble materials and to stabilize the oil in water and vice versa. Nowadays, considering the properties and the history of using the tragacanth in the traditional medicine, it is possible to create new opportunities for utilizingthis substance, especially in biomedicine [12].

Recently, some research works have been presented several reports about the formulating bioactive pastes based on the bioactive glass powder and natural polymers including 58S glass-sodium alginate [13], CaO-MgO-SiO_2-Na_2O-P_2O_5-CaF_2 bioactive glass-glycerol composite paste [14], and S53P4 glass–poly (ε-caprolactone-co-D,L-lactide) paste [15]. To the best of our knowledge, there is no report aboutpreparing the composite paste based on the 45S5 bioactive glass and gum tragacanth. Giving its inter-surface elasticity reduction properties, viscoelasticity, hydrophilicity, and biocompatibility, the gum tragacanth canbe a promising polymer matrix for preparing the composite pastes bythe bioactive glass.

This study has been aimed at formulating a biodegradable and biocompatible paste composed of the 45S5 bioactive glass and gum tragacanth, which hasgoodinjectability and bioabsorbability. These characteristics result insuitably flowing into the bone lesions, properly filling them up, and completely absorbingthe bone for a desired period of time. It is expected that the paste maintains its initial physical state after injection and has agood leaching resistance, which would be useful for the practical orthopedics. To find the optimal formulation, the various pastes were prepared by different concentrations of the tragacanth and P/L ratios. The prepared pastes then were characterized in terms of injectability, rheological behavior, swelling, and bioactivity.

2. MATERIALS AND METHODS

2.1. Materials

The reagent grade chemicals were (Sigma-Aldrich) used with no further purification.

2.2. Preparation of the 45S5 bioactive glass

According to the weight ratios of 45.0SiO_2, 24.5CaO, 24.5Na_2O, 6.0P_2O_5, the glass batch was prepared by mixing the raw materials in a planetary mill for 2 hours at 200rpm. At that moment, it was heated at 950° for 5 h in order to remove carbon impurities and then melted in a furnace (AZAR-1500) at 1400° for 2 h with aheating rate of 10 °/min. The resulting melt was quenched in the cold deionized water to produce the glass frit. Finally, the frit was milled in a planetary ball-mill (RETSCH-PM 400) at a speed of 250rpm for 3 hours to obtain the glass powder.

2.3. Characterization of the bioactive glass powder

Phase analysis was carried out by X-ray Spectrometer (XRD, Philips PW3710) with Cu-Kα radiation operating at 40kV and 30mA. To identify the chemical bonds and functional groups, Fourier transforminfrared (FTIR) spectra were recorded on a PerkinElmer Spectrum 400 instrument. For starting the experiment, 10mg of the powdered sample was mixed with 800mg of KBr and pressed into a disc, which was analyzed in the wavenumber range of 400-4000cm-1 with a 2 cm-1resolution . The specific surface area of the powder was measured using nitrogen gas absorption/desorption based onBET method on a BELSORP-mini II instrument.The pore volume and surface area were measured by Barret-Joyner-Halenda (BJH) technique on the isothermdesorption branch . The morphology and elemental composition of the glass particles were investigated by field-emission scanning electron microscopy (FESEM, Tescan Mira 3 LMU) equipped with energy dispersive X-ray spectroscopy (EDS, Bruker, Quantax 200).

2.4. Preparation of the injectable composites

Firstly, tragacanth aqueous solutions having concentrations of 2 and 4 w/v% were prepared by the gum tragacanth dissolving in the deionized water under

stirring to obtain a homogeneous solution. Thereafter, the composites were made readythrough simple mixing-spatulation of the tragacanth solution and bioactive glass powders in the different P/L ratios given in Table 1. It should be noted that the aforementioned ratios and concentrations were selected based on the workability of the resulting pastes. Clearly, the pastes with improper workability were notconsidered for further study.

TABLE 1. The injectable composite formulations

Sample	Tragacanth concentration (w/v%)	P:L (g:ml)
TG4-2	4.0	2.0: 1.0
TG4-1.8	4.0	1.8: 1.0
TG4-1.5	4.0	1.5: 1.0
TG2-2.5	2.0	2.5: 1.0
TG2-2.3	2.0	2.3: 1.0
TG2-2	2.0	2.0: 1.0

2.5. Rheological properties of the injectable composites

The rheological properties of the injectable composites were scrutinized in rotation and oscillation modes using an MRC 301 Anton Paar Rheometer with parallel plates. To this end, 3gr of the prepared composite was entered into the center of the lower plate, while the gap between the plates was adjusted to 1mm. The static parameters were estimatedby controlling the shear rate. It increased according to a predetermined shear rate-time program from 0 s^{-1} to 1000 s^{-1} in 180s and then reducedto zero duringthe same time. The shear stress and viscosity curves were plotted versusthe shear rate. The sweeping curves formed a hysteresis loop in the shear stress-shear rate plot, which its area is proportional to thixotropy of the system. The yield stress and the loop's area were calculated using the Anton Paar-Rheoplus software.

In order tostudy the viscoelastic properties of the injectable composites, the experiments were also implementedin the dynamic mode. The storage modulus (G') and loss modulus (G") were plotted as a function of the angular frequency. At first, the test was conductedin a variable strain state at a constant frequency and temperature to obtain the maximum strain in the linear viscoelastic region. The measurements then were fulfilled at a constant strain of 0.01% and variable frequency of 0.1-100 s-1 to obtain the complex viscosity as a function of angular frequency.

2.6. Injectability of the composites

For this purpose, the prepared composites were got involvedinto 3 and 5ml syringes. The syringes were attached to a cubic box and then were put under compression at a speed of 15mm/min in a SANTAM STM-20 universal strength machine. The curves of the applied force against displacement were recorded and the injection percentage (I%) was measured according to the formula [16]:

$$I(\%) = \frac{W_{ip}}{W_{np}} \times 100 \quad (1)$$

WhereW_{ip} and W_{np} denotethe injected andinitial mass, respectively.

2.7. Bioactivity and apparent stability of the composites

To study the in vitrobehavior of the prepared injectable composites, 1.0g of the composite was soaked in 100ml of simulated body fluid (SBF) solution. The samples were stored in a shaker-incubator at 37° for 14 days. During this interval, the apparent changes on the composites were recordedby means of a digital camera. Based on the variations in the weight of the composites, the degradation percent (D%) was calculated as follows [17]:

$$D(\%) = \frac{W_d - W_f}{W_d} \times 100 \quad (2)$$

Where W_i and W_f denotethe weight of the dried composite andthe weight of composite after being soaked in the SBF, respectively. In Addition, the swelling percent (S%) of the composites was determined using the equation [17]:

$$S(\%) = \frac{W_s - W_d}{W_s} \times 100 \quad (3)$$

Where W_d and W_s is the weight of the composite before and after immersion in the SBF, correspondingly.

The apatite formation on the surface of the composites as a criterion for in vitro bioactivity was evaluated using the observations created by XRD, FTIR, and SEM-EDX.

During the immersion of the composites into the SBF, the pH fluctuations were recorded using pH meter (Metrohm 827 pH Lab). Moreover, the concentration of calcium, phosphorus, and silicon ions were measured by inductively coupled plasma (ICP) spectroscopy on an Optima 8000 spectrometer.

2.8. Statistical analysis

Each experimentwas repeated three times and the data were reported as the mean ± standard deviation (SD). The results were statistically analyzed using one-way analysis of variance (ANOVA) method in which the differences at p-value<0.05 were statistically considered significant.

3. RESULTS AND DISCUSSION

3.1. Bioactive glass powder

Figure1(a) displays the XRD pattern of the glass powder prepared by the melting-quenching method. The pattern clearly shows a broad diffraction characteristic of the amorphous phase. There cannot be found any diffraction

related to possible crystal impurities suggesting the high phase purity of the prepared glass powder.

Figure1(b) shows the FTIR spectrum of the BG powder. The absorption bands sited at ~497cm^{-1} is the characteristic of the silicate network assigning to the Si—O—Si symmetric bending in silicate tetrahedrons. The centered peak at ~733cm^{-1} is initiated fromthe symmetric stretching vibrations of Si—O—Si in the glass. The absorption peaks in the wavenumber range of 900–1200cm^{-1} are attributed to the Si—O—Si asymmetric stretching and P—O stretching vibrations. The peak at ~1450cm^{-1} because of C—O stretching vibrations recommends the presence of carbonate groups (CO_3^{-2}) in the glass. The broad peak centered at ~3491cm^{-1} is allocated to the stretching vibrations of O—H group in adsorbed water molecules [18, 19]. The unresolved bands in the spectrum endorse the amorphous structure of the glass powder, which is comprehended from XRD pattern.

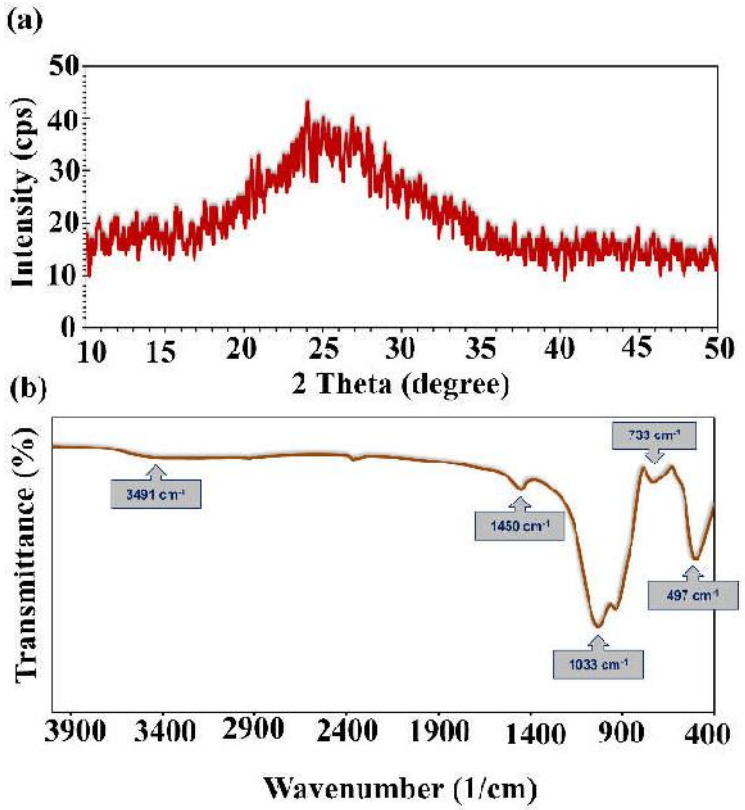

Figure 1. (a) XRD pattern and (b) FTIR spectrum of the melt-derived bioactive glass powders

Figure 2(a) shows FESEM micrograph of the glass powder. It clearly shows the glass particles having irregular morphologies with jagged and sharp edges. The powder mainly consists of the particles with sizes in the range of 0.3 to 3μm.

The EDS pattern of the glass powder is shown in Figure 2(b). The pattern illustrates the peaks related to Ca, Na, Si, O, and P as the main compositional elements of the glass. There is no peak interconnectedwiththe other elements in the EDS pattern.

The adsorption-desorption isotherm and the pore size distribution curve of the glass powder is shown in Figure 3.

The isotherm indicates atype V adsorption behavior together with atype H_1 hysteresis loop assigning to the mesoporous materials with low adsorption energy based on the IUPAC classifications [20]. According to the isotherm, it can be clarifiedthat at a low relative pressure region ($P/P_0<0.5$), the isotherms are relatively flat and theiradsorption and desorption entirely overlap. This is mainly due to the adsorption in the micropores. At a higher pressure region ($P/P_0>0.5$), the isotherms rapidly increase and form a lag loop, which is attributed to the capillary agglomeration phenomenonresponsible for filling the large mesopores and macropores [21].

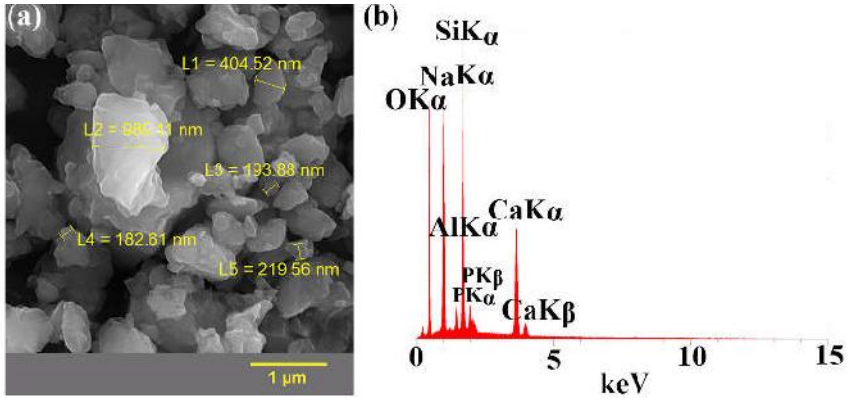

Figure 2. (a) SEM micrograph and (b) EDS pattern of the glass powders

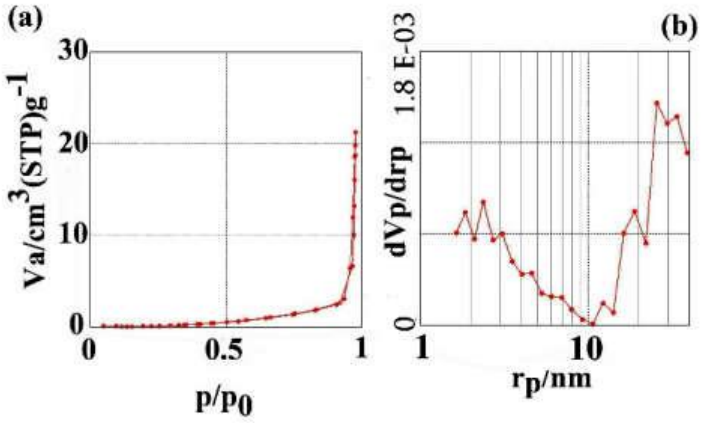

Figure 3. (a) N_2 adsorption-desorption isotherms, and (b) BJH pore size distribution curve for the glass powders

The specific surface area (S_{BET}) of the glass powder is equalto 0.29 $m^2.g^{-1}$, which is comparable to the values reported in the literature [22].

The average particle size (D_{BET}) of the powder is calculated by the following fundamental equation [20]:

$$D_{BET} = \frac{6000}{S_{BET} \times \rho} \quad (4)$$

Where S_{BET} is the specific surface area ($m^2.g^{-1}$)and ρ is the theoretical density of the glass particles ($g.cm^{-3}$) that is 2.65$g.cm^{-3}$ for the 45S5 bioactive glass. The average particle size of the glass powder is equalto 7.8 µm.

The Barrett-Joyner-Halenda (BJH) pore size distribution of the glass powders shows two broad peaks: one centered at ~2.5nm corresponds to the internal space of the particles and another at ~11.5nm, which is ascribed to the interparticle pores [21].

3.2. The paste characteristics

Figure 4(a) shows the curves related to theshear stress versus the shear rate for the composites formulated from the tragacanth solutions with different concentrations of 2.0 and 4.0 %. The sweeping curves form a hysteresis loop, which is presented the thixotropic behavior of the composites. Both composites show positive thixotropic behavior which means that the shear stress of the decreasing curve is less than that of the increasing curve at a constant shear rate. It can be concluded that using 2% tragacanth than 4% results in a greater thixotropy effect on te prepared composites, which is realized from the hysteresis loop's area.Another parameter describing the thixotropy is the flow behavior index (n), which tends to be 1.0 for Newtonian fluids and zero for non-Newtonian ones. It seems that by increasing the concentration of the tragacanth solution, n tends to be 1.0, which leads to decreasing the thixotropy [23].

The thixotropy degree (or level) is proportional to the required force for breaking down the internal structure formed owing to the interactions of the glass particles with the tragacanth. The larger the area of the hysteresis loop, the stronger the interparticle bonds are and the energy needed to break them. In the prepared composites, the destruction rate of the internal structure is more than its reconstruction rate. Referring to literature, the composite pastes made of the bioactive glass and hyaluronic acid polymeric solution show weak interparticle interactions along with the same destruction and reconstruction rates, which cause the non-thixotropicbehavior [23]. However, the composite pastes composed of the bioactive glass particles and sodium alginate showed similar thixotropic behavior towards the prepared composites in this study [24]. Figure 4(b) shows the viscosity variations as a function of the shear rate. When the shear velocity increases, the viscosity of the composites decreases. Therefore, all the composites show shear thinning behavior indicating that they easily flow at the stress beyond the yield one. This causes the composites to be injected well and remain homogeneous during injection process. This figure shows that at shear rates lower than $1s^{-1}$, the viscosity of the composites decreases with increasing the tragacanth concentration, while at shear rates above $100s^{-1}$, elevating the tragacanth concentration leads to increasing the viscosity. Figure 4(c) displays the plot of complex viscosity against the angular frequency. In both composite formulations, the viscosity decreases by increasing the angular frequency (at frequencies below 100 $rad.s^{-1}$) indicating that the composites behave as the non-Newtonian fluids. It can be also observed that the complex viscosity decreases by increasing the tragacanth concentration from 2.0 to 4.0 % at low frequencies, however, this behavior is totally reversed at frequencies above 5 $rad.s^{-1}$.

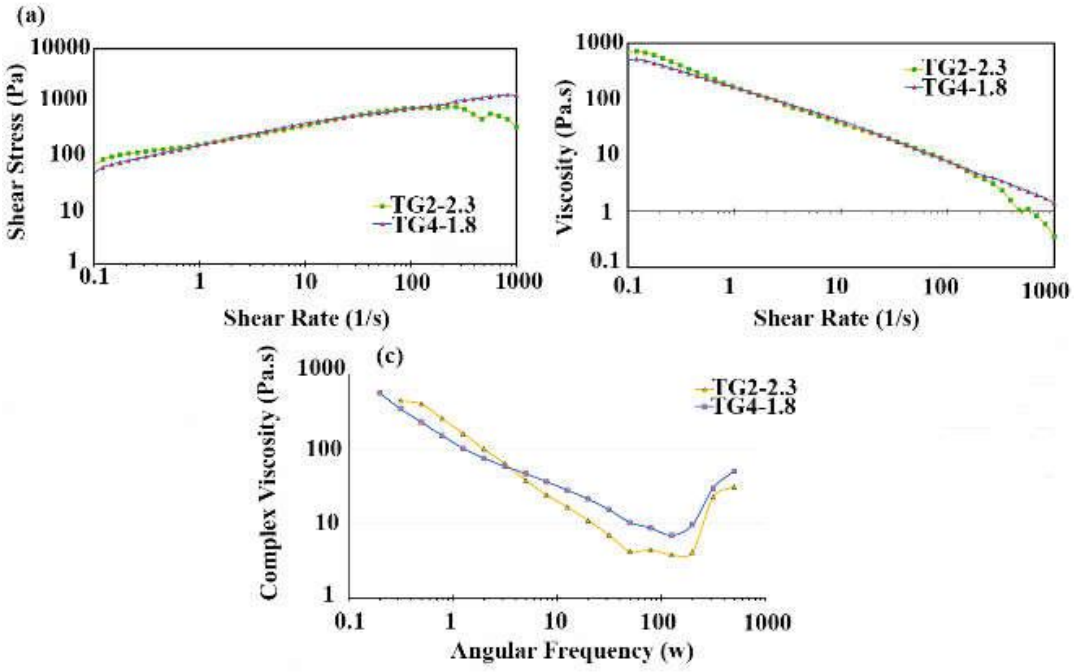

Figure 4. The curves of (a) shear stress vs. shear rate, (b) viscosity vs. shear rate; and (c) complex viscosity vs. angular frequency for the formulated composites

The oscillatory (dynamic) rheology test was performed in severalmodes includingvariable strain, frequency and time. In the mode of variable strain, the sample was exposed to an increasing strain and the plot of storage and loss modulus was recorded as a function of the strain. As shown in Fig. 5(a) and 5(b), at low strains, the storage and loss modulus are independent of the strain, but when it is increased, the modules begin to decrease at a critical point. The oscillatory rheology test can be accomplished in the linear region of the curve referred to as the linear viscoelastic region because at the strains above the linear strain the matter is destructed the interparticle bonds are broken. Therefore, the lowest possible strain (0.5%) was selected to continue the test. Figures 5(c) and 5(d) shows the variations in the storage and loss modulus for the composites made by different concentrations of the tragacanth. In the case of 4% tragacanth, the storage modulus is lower than the loss modulus at all frequencies, which is a clear sign of liquid behavior of the composite. In the composites composed of 2% tragacanth, the

storage module is higher than the loss modulus at the frequencies below 10 rad.s^{-1}, but it reverses at higher frequencies. This proposes that the viscous and elastic modulus of the composite depend on the frequency, thus, the external stress goes beyond yield stress at high frequencies and the composite becomes flowable.

The injection profiles of the prepared composites are presented in Figure 6. For all the composites, the force applied at the beginning of the injection rapidly increases in order to overcome the friction between the syringe and compositewalls. Subsequently, the injection continues with a constant force. It should be noted that sudden drop and variations onthe applied force can be related to the entrapped air into the composite. With the increase of the P/L ratio and tragacanth concentration, the injection force heightens, however, all specimens were completely injected except TG2-2.5. Due to the interconnections between the glass particles and the tragacanth solution, no phase separation is occurred in the formulated composites. Generally, all formulated composites can be injected at a force of less than 15N, which is a suitable value for the surgical purposes [23, 24].

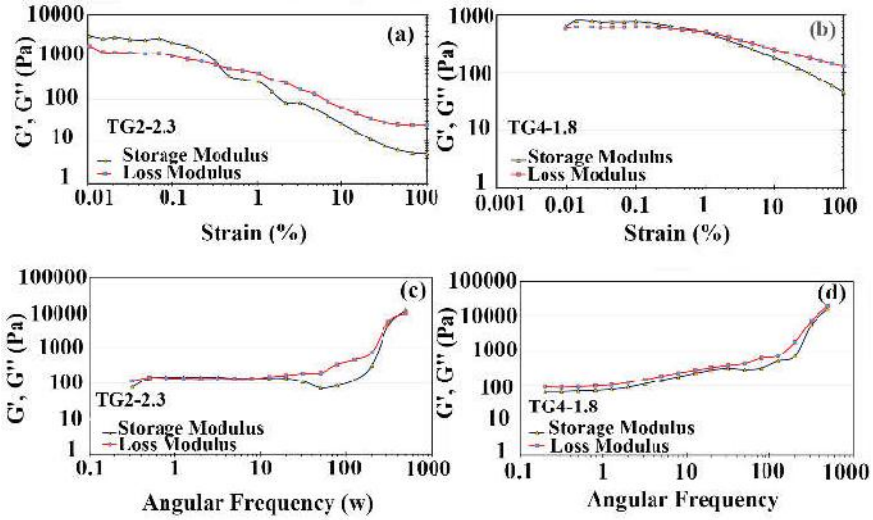

Figure 5. The curves of (a) storage/loss modulus vs. strain for TG 2-2.3, (b) storage/loss modulus vs. strain for TG 4-1.8, (c) storage/loss modulus vs. angular frequency for TG 2-2.3, and (d) storage/loss modulus vs. angular frequency for TG 4-1.8

According to what mentioned in the literature, the factors influencing the flowability of the injectable biomaterials are divided into four categories [25]:

(i) Test parameters including the syringe size, cannula size, injection length and the applied force rate;
(ii) Physics and chemistry of the fluid phase;
(iii) Solid phase characteristics such as morphology, particle size, distribution, powder permeability, and plastic limits;
(iv) Powder to liquid ratio (P/L).

Figures 7(a) and 7(b) show the photographs of the composites after injection andsoaking in the SBF (for 0.5 and 24 h), respectively. The swelling in the composites is clearly observed after being soaked in the SBF for 5 h. It seems that the apparent stability of the composites increases with rising the tragacanth concentration.

Figure 8 indicates the quantified results of the swelling and degradation. As can be seen, the composites formulated from 2% tragacanth show much more resistance against degradation and swelling. The injectable biomaterials having good injectability and leaching resistance are highly demanded for clinical applications.

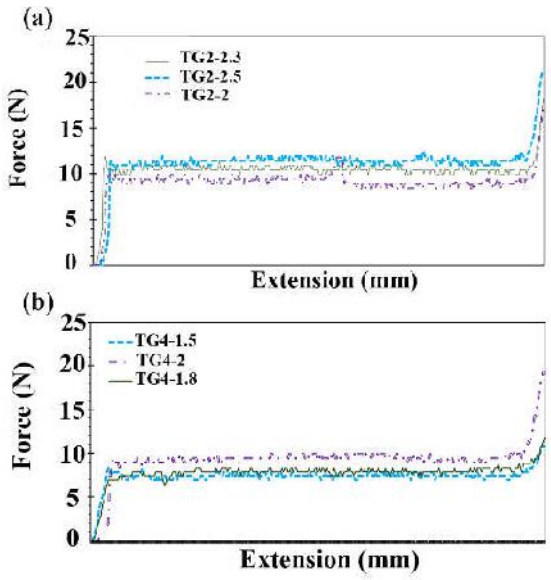

Figure 6. Injection profiles for the composites made of (a) 2% tragacanth, and (b) 4% tragacanth

When the injectable biomaterials are practically employed, they should withstand the high blood pressure and do not displacetothe other parts of the body [26].
It seems that the gum tragacanth induces the resistance against leaching and swelling in the formulated composite via increasing the viscosity and interparticle attractions and subsequently the chemical bonding to the glass particles. Firstly, the glass particles are surrounded by a few layers of the gum and then —COO^- and —OH^- functional groups in the tragacanth can electrostatically react with Ca^{2+} released from the surface of the glass particles and form strong bonds.

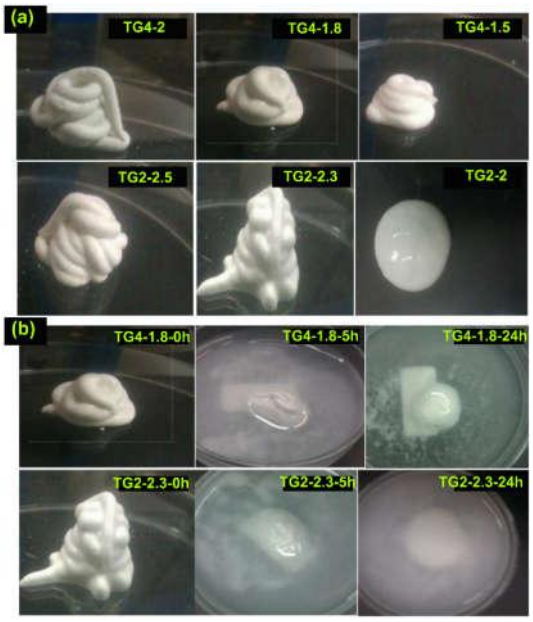

Figure 7. Photographs of the composites after (a) injection and (b) immersion in the SBF

Both glass-tragacanth and tragacanth-tragacanth interactions play important roles in the stability and resistance of the composite paste. In fact, if the internal structures are weak, they can be easily broken down by applying a shear stress and are re-created through removing it. In other words, it can be expressed that the rate of their destruction and reconstruction is equal. Nonetheless, the strong interactions between the glass particles and polymer (tragacanth) molecules produce thixotropy. Therefore, it can be concluded that the composites having higher thixotropy lead to a better structural stability in the body fluids [12, 16].
Figure 9 shows SEM micrographs of the TG2-2.3 and TG4-1.8 composites after immersion in the SBF for 7 and 21 days. The flower-likenanostructures formed on the surface of the composites are characteristic of the biological apatite.
The apatite nanostructures become much denser when the immersion time in the SBF isincreased. The formation of the bioactive apatite layer on the surface of TG4-1.8 composite after 7 days of immersion presentsthe improved bioactivity of the formulated composites compared tothe composite pastes based on the presence of the sodium alginate and bioactive glass nanoparticles, which has been reportedby Borhan et al. [24].
Figure 10 shows the EDS patterns of TG2-2.3 and TG4-1.8 composites after immersion in the SBF for 7 and 21 days.

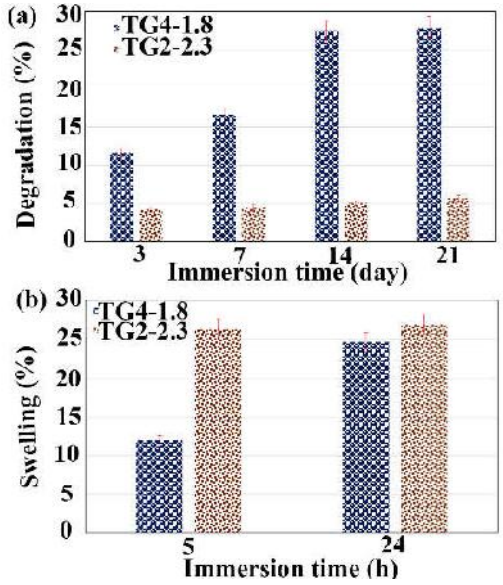

Figure 8. The percent of (a) degradation and (b) swelling in the composites due to immersion in the SBF

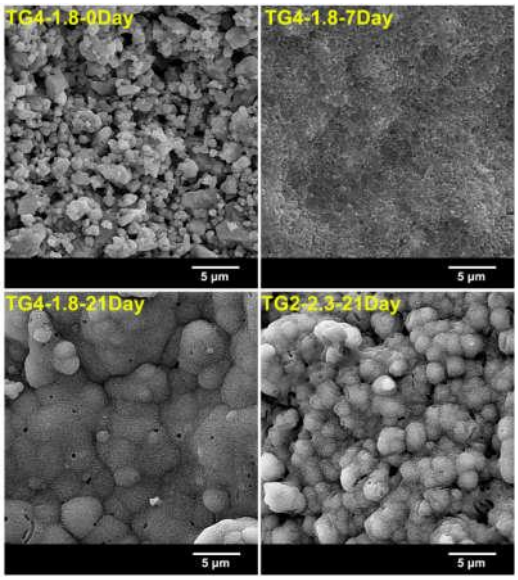

Figure 9. FESEM micrographs of the composites before and after immersion in the SBF

The patterns indicate increasing the Ca/P ratio in the composites because ofthe immersion time increasein the SBF and the tragacanth concentration enhancementup to 4%, which confirmsthe bioactivity improvement of the composites owing to the aforementioned factors.

The mechanism of the apatite formation has been described in details in literature [27]. During the initial days, an amorphous layer composed of $CaO\text{-}P_2O_5$ is deposited on the surface of the biomaterials, which then gradually turns into the crystalline and semi-crystalline apatite. Thisphenomenon is controlled by dissolution and deposition processes and depends on the saturation of the SBF solutionthrough biological ions. It is worthy to note that the saturation occurs through the dissolution of the glass particles and releasing Ca^{2+} and PO_4^{3-} into the SBF. The released calcium ions are replaced by H_3O^+ in the solution leading to increasingthe solution pH, which is the optimum condition for nucleation and crystallization of the biological apatite [27, 28].

Figure11(a) shows the XRD patterns of the TG2-2.3 and TG4-1.8 composites before and after immersion in the SBF for 21 days.

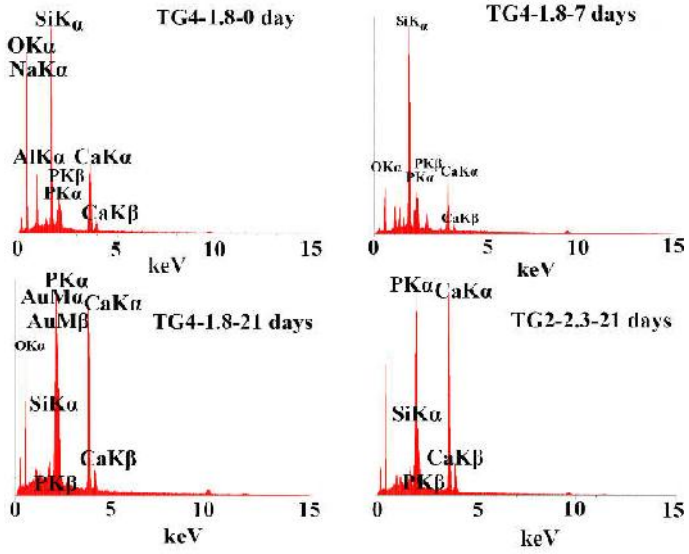

Figure 10. EDS patterns of the composites before and after immersion in the SBF

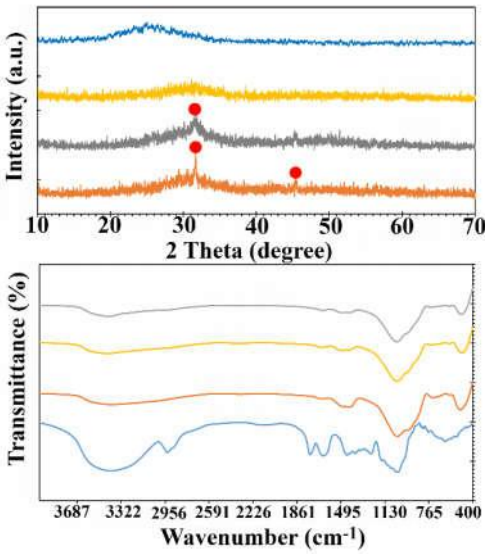

Figure 11. (a) XRD patterns and (b) FTIR spectra of the composites before and after immersion in the SBF for 21 days

Before immersion, the broad diffraction pattern pertains to the glass powder polymer (tragacanth) with an amorphous structure. After 14 days of the immersion, the peak appeared at 2θ= 31.8°, which is related to (211) diffraction plane in the hydroxyapatite crystal system (JCPDS No.00-09-0432). The peak with low intensity at 2θ= 46.8° is also related to the (222) diffraction plane of the apatite [29]. The low intensity and broadness of the aforementioned bands suggest that the newly formed hydroxyapatite is low crystalline, or the size of the crystals is in the nanometer range or a combination of both.

Figure 11(b) displays the FTIR spectra of TG2-2.3 and TG4-1.8 composites before and after immersion in the SBF for 21 days. Before immersion in the SBF, the peaks at ~500, 1025, 1420, and 3381cm^{-1} are assigned to the Si—O—Si symmetric bending, Si—O—Si stretching or P—O stretching, stretching vibrations of carbonate group and stretching vibrations of O—H group in the bioactive glass powder, respectively. The centered characteristic peaks at 3425, 2931, 1035, and 635cm^{-1} are attributed to the O—H stretching, C—H asymmetric stretching,

C—O stretching and C—O—C stretching vibrations in the gum tragacanth, correspondingly.

4. CONCLUSION

The injectable composites were fabricatedfromthe 45S5 bioactive glass powder and gum tragacanth and modified using different tragacanth concentrations and powder to liquid ratios. The formulated composites showed the maximum injection force of 15N, positive thixotropic behavior, optimum swelling percentage (~12%), and improved bioactivity. The results emphasized the optimal injectability, degradation/swelling resistance, and bioactivity of the composites formulated by 2% tragacanth with P/L ratio of 2.3. This recommends a synergy betweenthe 45S5 bioactive glass and gum tragacanth leading to the formation of an integrated composite structure with desirable physicomechanical properties required for the practical biomedical applications.

ACKNOWLEDGMENT

The Authors would like to thanks the Materials and Energy Research Center for hisfinancial support under the grant No. 99385001.

REFERENCES

1. Mano, J.F., Sousa, R.A., Boesel, L.F., Neves, N.M. and Reis, R.L., "Bioinert, biodegradable and injectable polymeric matrix composites for hard tissue replacement: state of the art and recent developments", ***Composites Science and Technology*** Vol. 64, (2004), 789-817.
2. González, C., Vilatela, J.J., Molina-Aldareguía, J.M., Lopes, C.S. and Llorca, J., "Structural composites for multifunctional applications: Current challenges and future trends", ***Progress in Materials Science***, Vol. 89, (2017), 194-251.
3. Venkatesan, J., Bhatnagar, I., Manivasagan, P., Kang, K.H. and Kim, S.K., "Alginate composites for bone tissue engineering: A review", ***International Journal of Biological Macromolecules***, Vol. 72, (2015), 269-281.
4. Baino, F., Fiorilli, S. and Vitale-Brovarone, C., "Bioactive glass-based materials with hierarchical porosity for medical applications: Review of recent advances", ***Acta Biomaterialia,*** Vol. 42, (2016), 18-32.
5. Miguez-Pacheco, V., Hench, L.L. and Boccaccini, A.R., "Bioactive glasses beyond bone and teeth: Emerging applications in contact with soft tissues", ***Acta Biomaterialia,*** Vol. 13, (2015), 1-15.
6. Jones, J.R., "Review of bioactive glass: From Hench to hybrids", ***Acta Biomaterialia,*** Vol. 23, (2015) s53-s82.
7. Park, S.B., Lih, E., Park, K.S., Joung, Y.K. and Han, D.K., "Biopolymer-based functional composites for medical applications, ***Progress in Polymer Science***, Vol. 68, (2017), 77-105.
8. Rao, S.H., Harini, B., Shadamarshan, R.P.K., Balagangadharan, K. and Selvamurugan, N.," Natural and synthetic polymers/bioceramics/bioactive compounds-mediated cell signalling in bone tissue engineering", ***International Journal of Biological Macromolecules***, Vol. 110, (2018), 88-96.
9. Zhao, W., Jin, X., Cong, Y. Liu, Y. and Fu, J., "Degradable natural polymer hydrogels for articular cartilage tissue engineering", ***Journal of Chemical Technology and Biotechnology***, Vol. 88, (2013), 327-339.
10. Gyles, D.A., Castro, L.D., Carréra Silva, J.O. and Ribeiro-Costa, R.M., "A review of the designs and prominent biomedical advances of natural and synthetic hydrogel formulations", ***European Polymer Journal***, Vol. 88, (2017), 373-392.
11. Ghayempour, S. and Montazer, M.A, "modified microemulsion method for fabrication of hydrogel Tragacanth nanofibers", ***International Journal of Biological Macromolecules***, Vol. 115, (2018), 317-323.
12. Rahmani, Z., Sahraei, R. and Ghaemy, M., "Preparation of spherical porous hydrogel beads based on ion-crosslinked gum tragacanth and graphene oxide: Study of drug delivery behavior", ***Carbohydrate Polymers***, Vol. 194, (2018), 34-42.
13. Sohrabi, M., Hesaraki, S., and Kazemzadeh, A., " Injectable Bioactive Glass/Polysaccharide Polymers Nanocomposites for Bone Substitution", ***Key Enginnering and Materials***, Vol. 614, (2014), 41-46.
14. Tulyaganov, D., Abdukayumov, K., Ruzimuradov, O., Hojamberdiev, M., Ionescu, E., and Riedel, R., "Effect of alumina incorporation on the surface mineralization and degradation of a bioactive glass (CaO-MgO-SiO_2-Na_2O-P_2O_5-CaF_2)-glycerol paste", ***Materials***, Vol. 10, (2017), 1324.
15. Aho, A.J., Tirri, T., Kukkonen, J., Strandberg, N., Rich, J., Seppälä, J., and Yli-Urpo, A., "Injectable bioactive glass/biodegradable polymer composite for bone and cartilage reconstruction: Concept and experimental outcome with thermoplastic composites of poly(ε-caprolactone-co-D,L-lactide) and bioactive glass S53P4", ***Journal of Materials Science: Materials in Medicine***, Vol. 15, (2004), 1165–1173.
16. Borhan, S., Hesaraki, S., Behnamghader, A.A., and Ghasemi, E., "Rheological evaluations and in vitro studies of injectable bioactive glass-polycaprolactone-sodium alginate composites", ***Journal of Materials Science: Materials in Medicine***, Vol. 27, (2016), 137.
17. Nwe, N., Furuike, T., and Tamura, H., "The mechanical and biological propertiesof chitosan scaffolds for tissue regeneration templates are significantlyenhanced by chitosan from Gongronellabutleri", ***Materials***, Vol. 2, (2009), 374–398.
18. Shamsi, M., Karimi, M., Ghollasi, M., Nezafati, N., Shahrousvand, M., Kamali, M., and Salimi, A., "In vitro proliferation and differentiation of human bone marrow mesenchymal stem cells into osteoblasts on nanocomposite scaffolds based on bioactive glass ($64SiO_2$-$31CaO$-$5P_2O_5$)-poly-l-lactic acid nanofibers fabricated by electrospinning method", ***Materials Science and Engineering C***, Vol. 78, (2017), 114-123.
19. Karimi, M., Hesaraki, S., Alizadeh, M., and Kazemzadeh, A., "A facile and sustainable method based on deep eutectic solvents toward synthesis of amorphous calcium phosphate nanoparticles: The effect of using various solvents and precursors on physical characteristics", ***Journal of Non-Crystalline Solids***, Vol. 443 (2016) 59–64.
20. Karimi, M., Hesaraki, S., Alizadeh, M. and Kazemzadeh, A. , "Synthesis of calcium phosphate nanoparticles in deep-eutectic choline chloride–urea medium: Investigating the role of synthesis temperature on phase characteristics and physical properties", ***Ceramics International***, Vol. 42, (2016), 2780–2788.
21. Koike, N., Ikuno, T., Okubo, T, and Shimojima, A., "Synthesis of monodisperseorganosilica nanoparticles with hollow interiors and porous shells using silica nanospheres as templates", ***Chemical Communications***, Vol. 49, (2013), 4998.
22. Faure, J., Drevet, R., Lemelle, A., Ben Jaber, N., Tara, A., Btaouri, H.E., and Benhayoune, H., "A new sol-gel synthesis of 45S5 bioactive glass using an organic acid as catalyst", ***Materials Science and Engineering C***, Vol. 47, (2015), 407-412.

23. Sohrabi, M., Hesaraki, S., Kazemzadeh, A., and Alizadeh, M., "Development of injectable biocomposites from hyaluronic acid and bioactive glass nano-particles obtained from different sol–gel routes", ***Materials Science and Engineering C***, Vol. 33, (2013), 3730-3744.
24. Borhan, S., Hesaraki, S., Behanamghader, A.A., and Ghasemi, E., "Injectable bone paste biocomposite based on melt-derived bioactive glass and sodium alginate natural polymer", ***Journal of the Australian Ceramic Society***, Vol. 51, (2015), 99-108.
25. Habib, M., Baroud, G., Gitzhofer, F., and Bohner, M., "Mechanisms underlying the limited injectability of hydraulic calcium phosphate paste", ***Acta Biomaterialia***, Vol. 4, (2008), 1465-1471.
26. Gabbai-Armelin, P.R., Cardoso, D.A., Zanotto, E.D., Peitl, O., Leeuwenburgh, S.C.G., Jansen, J.A., Renno, A.C.M., and van den Beucken, J.J.J.P., "Injectable composites based on biosilicate® and alginate: handling and in vitro characterization", ***RSC Advances***, Vol. 4, (2014), 45778-45785.
27. Karimi, M., Hesaraki, S., and Nezafati, N., "In vitro biodegradability–bioactivity-biocompatibility and antibacterial properties of SrF_2 nanoparticles synthesized by one-pot and eco-friendly method based on ternary strontium chloride-choline chloride-water deep eutectic system", ***Ceramics International***, Vol. 44, (2018), 12877–12885.
28. Hill, R., "An alternative view of the degradation of bioglass", ***Journal of Materials Science Letters***, Vol. 15, (1996), 1122-1125.
29. Karimi, M., Hesaraki, S., Alizadeh, M. and Kazemzadeh, A., "Time and temperature mediated evolution of CDHA from ACP nanoparticles in deep eutectic solvents: Kinetic and thermodynamic considerations", ***Materials and Design***, Vol. 122 (2017), 1–10.
30. Karimi, M., Jodaei, A., Sadeghinik, A., Rastegar Ramsheh, M., Mohammadi Hafshejani, T., Shamsi, M., Orand, F. and Lotfi, F., "Deep eutectic choline chloride-calcium chloride as all-in-one system for sustainable and one-step synthesis of bioactive fluorapatite nanoparticles", ***Journal of Fluorine Chemistry***, Vol. 204, (2017), 76–83.